

# Stellar mass loss, rotation and the chemical enrichment of early-type galaxies

Antonio Pipino,<sup>1,2★</sup> Cristina Chiappini,<sup>3,4</sup> Genevieve Graves<sup>5</sup>  
and Francesca Matteucci<sup>4,6</sup>

<sup>1</sup>*Physics & Astronomy, University of Southern California, Los Angeles, CA 90089-0484, USA*

<sup>2</sup>*Astrophysics, University of Oxford, Denys Wilkinson Building, Keble Road, Oxford OX1 3RH*

<sup>3</sup>*Observatoire de Genève, Université de Genève, 51 Chemin de Mailletes, CH1290 Sauverny, Switzerland*

<sup>4</sup>*INAF–Osservatorio Astronomico di Trieste, Via G.B. Tiepolo 11, I-34127 Trieste, Italy*

<sup>5</sup>*UCO/Lick Observatory, University of California, Santa Cruz, CA 95064, USA*

<sup>6</sup>*Dipartimento di Astronomia, Università di Trieste, Via G.B. Tiepolo 11, I-34127 Trieste, Italy*

Accepted 2009 March 25. Received 2009 March 13; in original form 2008 December 20

## ABSTRACT

We present a comparison between the [Ca,C,N/Fe]–mass relations observed in local spheroids and the results of a chemical evolution model which already successfully reproduces the [Mg/Fe]–mass and the [Fe/H]–mass relations in these systems. We find that the [Ca/Fe]–mass relation is naturally explained by such a model without any additional assumption. In particular, the observed underabundance of Ca with respect to Mg can be attributed to the different contributions from Type Ia and Type II supernovae to the nucleosynthesis of these two elements. For C and N, we consider new stellar yields that take into account stellar mass loss and rotation. These yields have been shown to successfully reproduce the C and N abundances in Milky Way metal-poor stars. The use of these new stellar yields produces a good agreement between the chemical evolution model predictions and the integrated stellar population observations for C. In the case of N, the inclusion of fast rotators and stellar mass-loss nucleosynthesis prescriptions improves our predictions for the slope of the [N/Fe] versus  $\sigma$  relation, but a zero-point discrepancy of 0.3 dex remains. This discrepancy cannot be removed, either by increasing the N yields or by assuming a larger amount of fast rotators in spheroids, because in both cases this leads to an overproduction of the N abundances in the gas phase in these galaxies at high redshift (e.g. the Lyman break galaxy MS 1512–cB58). This work demonstrates that current stellar yields are unable to simultaneously reproduce the large mean stellar  $\langle [N/Fe] \rangle$  ratios inferred from integrated spectra of elliptical galaxies in Sloan Digital Sky Survey and the low N abundance measured in the gas of high-redshift spheroids from absorption lines. However, since chemical evolution models for the Milky Way computed with the Geneva stellar yields constitute at present the only way to account for the N/O, C/O and  $^{12}\text{C}/^{13}\text{C}$  abundance ratios observed in very metal-poor halo stars, it seems reasonable to suggest that there may be uncertainties in either the inferred stellar or gas-phase N abundances at the level of  $\sim 0.3$  dex.

**Key words:** stars: rotation – galaxies: abundances – galaxies: elliptical and lenticular, cD – galaxies: formation – galaxies: individual: MS 1512–cB58 – galaxies: stellar content.

## 1 INTRODUCTION

Abundance ratios can be used to constrain both galaxy formation scenarios and stellar nucleosynthesis. So far, in studies of elliptical galaxies, abundance ratios have been used with the former aim.

Indeed, increasing evidence has accumulated over the past decade that the [Mg/Fe] ratio is supersolar in the cores of bright galaxies and increases with galactic mass (e.g. Faber, Worthey & Gonzalez 1992; Worthey, Faber & Gonzalez 1992). It is also well established that elliptical galaxies obey the mass–metallicity relation, namely the stars of the brighter spheroids are more metal rich than those of the less luminous ones (Carollo, Danziger & Buson 1993). These two relations, along with the evolution of the luminosity function

★E-mail: pipino@usc.edu

(e.g. Bundy et al. 2005) led to the so-called downsizing picture: more massive galaxies form faster and earlier than less massive ones (Matteucci 1994).

Unfortunately, due to the fact that we cannot resolve stars in elliptical galaxies and because of the uncertainties in modelling line-strength indices as a function of abundance ratios, elliptical galaxies have not yet been used to constrain stellar nucleosynthesis calculations. Up to now, such studies have been restricted to the Milky Way (MW; e.g. Chiappini, Matteucci & Meynet 2003a; Chiappini, Romano & Matteucci 2003b; Cescutti et al. 2006) and its satellites (e.g. Lanfranchi, Matteucci & Cescutti 2006, 2008 for dwarf spheroidals; Pompeia et al. 2008 for the Large Magellanic Cloud) and damped Lyman alpha (DLA) systems (e.g. Dessauges-Zavadsky et al. 2007).

As an example, metal-poor halo stars in the MW are observed to have high levels of N/O and C/O (Akerman et al. 2004; Spite et al. 2005; Fabbian et al. 2009). The observed trends in C/O and N/O versus O/H at very low metallicities cannot be reproduced by chemical evolution models in which standard yields are adopted (see Chiappini, Matteucci & Ballero 2005 for a detailed discussion). In fact, due to the very low metallicities of such stars, the high levels of N/O would have to be the result of nucleosynthesis in metal-poor massive stars, suggesting these objects must produce primary nitrogen in non-negligible quantities.<sup>1</sup> It has recently been shown that fast stellar rotation is a promising mechanism for producing primary nitrogen in metal-poor massive stars (e.g. Meynet, Ekström & Maeder 2006; Hirschi 2007, hereafter H07). Chemical evolution models which include the yields of fast rotating models at low metallicity ( $Z = 10^{-8}$  by mass) can account for the observations in normal metal-poor halo stars (Chiappini et al. 2006a,b, 2008).

In principle, there is no reason why such fast rotators should occur only in the MW halo. These stars could also have left their imprints in DLAs and sub-DLAs (the most metal poor DLAs found at present). In fact, Pettini et al. (2008) find that these metal-poor high-redshift systems also show large C/O and N/O ratios, compatible with what is found in the MW halo. Given these successes, it is important to determine whether the stellar yields adopted in Chiappini et al. (2006a) can also give consistent results for other systems whose star formation histories differ from that of the solar vicinity and the MW, such as DLAs (Chiappini et al., in preparation) and elliptical galaxies (this work).

The large number of galaxies observed in the recent Sloan Digital Sky Survey (SDSS; York et al. 2000) make it possible to construct very high signal-to-noise ratio (S/N) spectra for typical elliptical galaxies by stacking together the spectra of many similar objects. The resulting data are of high enough quality to enable the study of line-strength ratios for multiple different elements on a more robust basis (Graves et al. 2007). At the same time, Schiavon (2007) has produced a new class of stellar population models which take into account the effect of various abundance patterns. These models allow us to estimate not only the total metallicity, age and  $[\alpha/\text{Fe}]$  of galaxies, but also the relative abundances of several other elements, such as carbon, nitrogen and calcium.

Graves et al. (2007) find that many properties of the stellar populations in red sequence galaxies (such as age,  $[\langle\text{Fe}/\text{H}\rangle]$  and  $[\langle\text{Mg}/\text{Fe}\rangle]$ ) vary with galaxy velocity dispersion ( $\sigma$ ). In particular, more massive galaxies are typically older, more metal rich and more

enhanced in Mg, as predicted by the chemical evolution models of Matteucci (1994) and in agreement with previous work (e.g. Trager et al. 2000b; Bernardi et al. 2003; Nelan et al. 2005). Using the newly developed capabilities of the Schiavon (2007) models, they further measure  $[\langle\text{Ca}/\text{Fe}\rangle]$ ,  $[\langle\text{C}/\text{Fe}\rangle]$  and  $[\langle\text{N}/\text{Fe}\rangle]$ . They find that Ca scales with Fe and, more surprisingly, that  $[\langle\text{C}/\text{Fe}\rangle]$  and  $[\langle\text{N}/\text{Fe}\rangle]$  increase with  $\sigma$  more strongly than  $[\langle\text{Mg}/\text{Fe}\rangle]$  does.

These results are crucial new constraints to study the role played by stars of different masses in the chemical enrichment of elliptical galaxies. This investigation aims at reproducing and understanding these abundance trends by means of a self-consistent chemical evolution model, whose predictions already match many previous observations. In this way we can, for the first time, use several abundance ratios measured in the stars of elliptical galaxies as constraints on nucleosynthesis calculations.

This paper is organized as follows. We first review the observational data and their uncertainties in Section 2, then present the main ingredients of our chemical evolution models in Section 3. In Section 4, we present our results and then summarize our main conclusions in Section 5.

## 2 OBSERVATIONS

### 2.1 The data

Graves et al. (2007) use a sample of  $\sim 6000$  galaxies from the SDSS main galaxy survey (Strauss et al. 2002) to determine the typical stellar population properties of elliptical galaxies as a function of  $\sigma$ . Their sample compares the stellar populations of quiescent elliptical galaxies (those with no emission lines in their spectra) to those of elliptical galaxies that host emission from low-ionization nuclear emission-line regions (LINERs). In this work, we are only interested in quiescent galaxies. Graves et al. sort galaxies into six  $\sigma$  bins, then stack the spectra of the galaxies in each bin to obtain very high S/N mean spectra. They then measure the strength of multiple absorption features in the spectra (using the Lick/IDS index system pioneered by Burstein et al. 1984) and use the models of Schiavon (2007) to convert the line strengths into measured values of mean, luminosity-weighted age,  $[\langle\text{Fe}/\text{H}\rangle]$ ,  $[\langle\text{Mg}/\text{Fe}\rangle]$ ,  $[\langle\text{Ca}/\text{Fe}\rangle]$ ,  $[\langle\text{C}/\text{Fe}\rangle]$  and  $[\langle\text{N}/\text{Fe}\rangle]$  for the stellar populations.

In agreement with many previous authors, Graves et al. find that age,  $[\langle\text{Fe}/\text{H}\rangle]$  and  $[\langle\text{Mg}/\text{Fe}\rangle]$  all increase with  $\sigma$  (see their table 8 for a detailed comparison with previous results). In particular, they find that  $[\langle\text{Mg}/\text{Fe}\rangle]$  ranges from +0.13 to +0.26 as  $\sigma$  goes from 100 to 250  $\text{km s}^{-1}$ . They furthermore find that  $[\langle\text{Ca}/\text{Fe}\rangle]$  has only very weak dependence on  $\sigma$  and is nearly solar for all galaxies, with values in the range  $-0.01 < [\langle\text{Ca}/\text{Fe}\rangle] < +0.03$  for galaxies with  $100 < \sigma < 250 \text{ km s}^{-1}$ .

Some of the most interesting results from the Graves et al. study, and the ones which motivated this analysis, were the observed trends in  $[\langle\text{C}/\text{Fe}\rangle]$  and  $[\langle\text{N}/\text{Fe}\rangle]$ . Both of these elements show strong enhancement with increasing  $\sigma$  (see Figs 1 and 2).

An overabundance of C and N in more massive ellipticals has been suggested by previous authors, but strong evidence has been lacking and there has been considerable confusion in the literature. The first hints came from Trager et al. (2000a)'s analysis of a sample of local ellipticals. They suggested that, in order to best fit their absorption line measurements for elliptical galaxies, C should be enhanced along with Mg and possibly O. Trager et al. therefore included C (as well as N) in the group of 'enhanced' elements when constructing their stellar population models but did not attempt to quantitatively measure  $[\langle\text{C}/\text{Fe}\rangle]$  or  $[\langle\text{N}/\text{Fe}\rangle]$ . Later,

<sup>1</sup> At least a factor of a few hundred more than what was already predicted by the models of (Meynet & Maeder 2002, hereafter MM02) with rotational velocities of 300  $\text{km s}^{-1}$  (see Chiappini et al. 2005 for details).

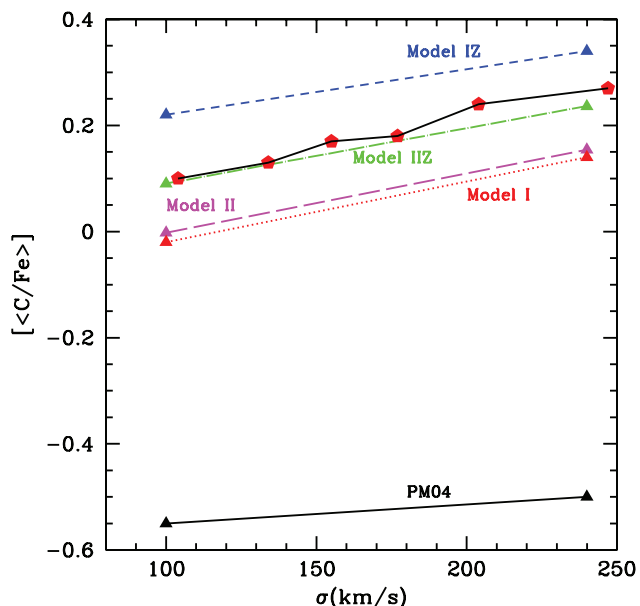


**Figure 1.** Mass-weighted  $[C/Fe]$  as a function of galactic velocity dispersion predicted by PM04 (triangles linked by a solid line) and models I (dotted line), IZ (short-dashed line), II (long-dashed line) and IIZ (short-dash-dotted line) compared to the observed relation found by Graves et al. (2007, pentagons linked by a solid line).

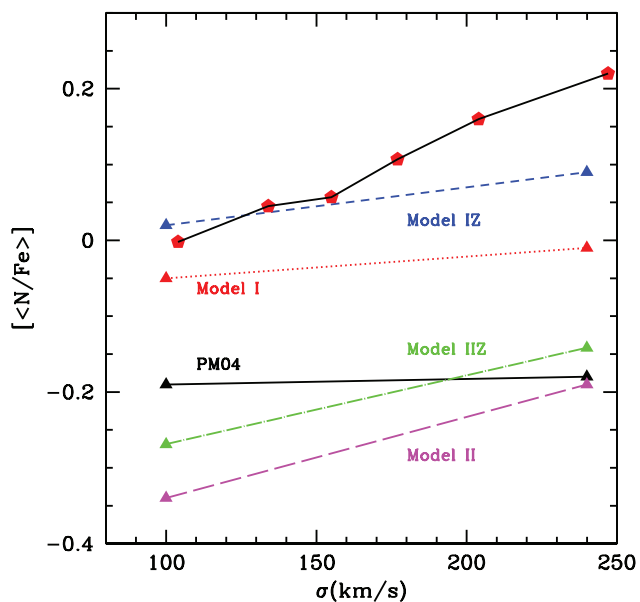


**Figure 2.** Mass-weighted  $[N/Fe]$  as a function of galactic velocity dispersion predicted by PM04 (triangles linked by a solid line) and models I (dotted line), IZ (dashed line), II (long-dashed line) and IIZ (short-dash-dotted line) compared to the observed relation found by Graves et al. (2007, pentagons linked by a solid line).

Sanchez-Blazquez et al. (2003) found a positive correlation between the strength of a CN absorption band and  $\sigma$ , which they interpreted as evidence for further enhancement in C and N with increasing  $\sigma$ . They did not attempt a quantitative conversion into abundance ratios.

Sanchez-Blazquez et al. further presented some evidence that galaxies in denser environments were somewhat less enriched in C and N with respect to their low-density counterparts. However,

Toloba et al. (2009) have recently claimed that this correlation disappears if one uses an NH feature at shorter wavelength. To further complicate matters, Clemens et al. (2006) corroborate the environment correlation proposed by Sanchez-Blazquez et al., but find an *anticorrelation* of  $[C/H]$  with galactic mass, in conflict with the other studies reported here.

The Graves et al. (2007) results are based on a large, homogeneous data set and take advantage of new advances in stellar population modelling. Furthermore, Graves & Schiavon (2008) have tested their method on integrated spectra of MW globular clusters. For a small number of clusters,  $[C/Fe]$  and  $[N/Fe]$  have been measured in spectra of individual cluster stars. The latter authors demonstrate that the values of  $[C/Fe]$  and  $[N/Fe]$  measured in integrated cluster spectra using their method match the average abundance determinations from individual cluster stars to within  $\pm 0.04$  dex. We therefore consider their abundance measurements to be reliable. However, the reader should bear in mind that there is not yet a consensus on C and N abundances in elliptical galaxies.

## 2.2 Uncertainties in deriving $[C/Fe]$ and $[N/Fe]$ from integrated spectra

The key results of this analysis consist of a comparison of the observed values of  $[C/Fe]$  and  $[N/Fe]$  from Graves et al. (2007) versus those obtain from chemical evolution models. In this context, it is important to review the uncertainties in the derivation of  $[C/Fe]$  and  $[N/Fe]$  using the method of Graves & Schiavon (2008). We list these in order of their likely importance, from most to least important.

(i) *Modelling  $[N/Fe]$  using a CN molecular absorption feature.* The abundance modelling process used in Graves et al. (2007) uses a CN molecular absorption feature to determine  $[N/Fe]$ , after  $[C/Fe]$  has been fixed based on a  $C_2$  feature (see Graves & Schiavon 2008 for details). This means that the measured value of  $[N/Fe]$  depends on the accuracy of the  $[C/Fe]$  determination and therefore has a larger associated uncertainty than the other abundance ratio measurements. In Graves & Schiavon (2008), this method is tested in globular clusters and is shown to reproduce the average  $[N/Fe]$  determined from individual cluster stars to within 0.04 dex. This suggests that the modelling process is accurate, however, the test has only been performed on two globular clusters to date. Recently, Toloba et al. (2009) suggested that the N abundance does not strongly correlate with mass by using a NH feature in the near-ultraviolet (UV), which may be a cleaner discriminant of N abundance. However, Toloba et al. did not attempt any conversion between the index and the actual N abundance, therefore, we cannot use their data as a further constraint for our models.

(ii) *Uncertainty in the  $[O/Fe]$  abundance.* The  $[C/Fe]$  and  $[N/Fe]$  stellar abundance ratios are measured using the  $C_2 4668$  and  $CN_1$  molecular absorption features. Both of lines are sensitive to the abundance of O, which competes with the formation of  $C_2$  and CN. Thus higher O abundances will inhibit the formation of these molecules, resulting in weaker absorption features for fixed values of  $[C/Fe]$  and  $[N/Fe]$ . Unfortunately, O is currently unmeasurable in spectra of unresolved stellar populations. The abundances presented here are computed assuming solar O/Fe abundance ratio (i.e.  $[O/Fe] = 0.0$ ). However, early-type galaxies are known to be enhanced in  $\alpha$ -elements and likely have supersolar  $[O/Fe]$ . Accounting for the likely supersolar  $[O/Fe]$  will have the effect of *increasing* the measured stellar values of  $[C/Fe]$  and  $[N/Fe]$ , since larger C and N abundances will be needed to produce the same

absorption line strengths. As will be shown, the measured values of [C/Fe] and [N/Fe] are relatively high already. Furthermore, recent evidence from MW bulge stars suggests that [O/Fe] may be  $\sim$ solar for metal-rich bulge stars, despite their supersolar values of [Mg/Fe] (Fulbright, McWilliam & Rich 2007).

(iii) *The effects of rotation on evolutionary tracks.* There is some indication that stars with fast rotation have bluer evolutionary tracks than non-rotating stars of the same mass (Meynet, private communication), which will affect the stellar population analysis of these galaxies. However, while the temperature differences should have a substantial impact on age measurements, they should have little effect on the abundance ratios. This can be seen in the comparison of solar-scale and  $\alpha$ -enhanced evolutionary tracks in Schiavon (2007) and Graves et al. (2007), where turn-off temperatures and age measurements are strongly affected but abundance ratios are not.

(iv) *The effects of emission infill.* The galaxies in Graves et al. (2007) have been selected to have no detectable emission lines in their spectra, based on the strong emission lines at H $\alpha$  and [O II] $\lambda$ 3727. Thus the effects of H $\delta$  emission are unlikely to substantially contaminate the CN absorption index in these galaxies. For galaxies in Graves et al. (2007) that did contain significant emission (not used in this work), variations in the emission infill correction resulted in differences of  $< 0.01$  dex in [(N/Fe)].

(v) *Lick index zero-point offsets.* The galaxy data from Graves et al. (2007) are not zero-point shifted to the original Lick/IDS system. However, this should not have a significant effect on the abundance determinations. Both the SDSS data and the Schiavon (2007) stellar population models used to interpret them are based on flux-calibrated spectra. Schiavon (2007) demonstrates that the zero-point offsets between Lick indices measured in flux-calibrated spectra are extremely small (see fig. 2 of that work), with the exception of the indices Fe5015, Fe4383, H $\gamma_A$  and H $\delta_A$ , none of which are used in abundance analysis of Graves et al.

### 3 THE MODEL

#### 3.1 The Pipino & Matteucci (2004) chemical evolution model

The adopted chemical evolution model is an updated version of the multizone model of Pipino & Matteucci (2004, hereafter PM04). We calculate the evolution of element abundances by means of the equation of chemical evolution (see e.g. Matteucci & Greggio 1986 for a comprehensive discussion of this equation). The initial mass function (IMF)  $\phi(m) \propto m^{-(1+x)}$  is normalized to unity in the mass interval 0.1–100  $M_\odot$ . We adopt an IMF with  $x = 1.35$  (Salpeter 1955).

We adopt the following law for the star formation rate (SFR):

$$\psi(t) = \nu t M_{\text{gas}}(t), \quad (1)$$

where the SFR  $\psi(t)$  is assumed to be proportional to the gas mass via a constant  $\nu$  which represents the star formation efficiency. We assume  $\nu = \nu_{\text{PM04}}$ , i.e. as in model II of PM04 where  $\nu$  is an increasing function of the galactic mass.

The star formation history of a model galaxy is determined by the interplay between the infall time-scale, the star formation efficiency and the onset of the galactic wind [i.e. the energetic feedback from supernovae (SNe) and stellar winds]. We assume that  $\psi = 0$  after the development of the galactic wind.

A fundamental component of this model is the detailed calculation of SN explosion rates. For Type Ia SNe, we assume a progenitor model made of a C–O white dwarf plus a red giant (Greggio &

Renzini 1983; Matteucci & Greggio 1986). The predicted Type Ia SN explosion rate is constrained to reproduce the present day observed value (Mannucci et al. 2008).

Here we adopt the same formulation for the feedback as in Pipino et al. (2002), to which we refer the reader. In brief, we consider a  $\sim 20$  per cent mean efficiency in energy transfer from the SN into the interstellar medium. In addition, we define the onset of the galactic wind ( $t_{\text{gw}}$ ) as the time at which the energy input by SNe exceeds the gas binding energy (for details see Pipino et al. 2002; PM04). The wind carries out the residual gas from the galaxies, thus inhibiting further star formation.

In PM04, we simulated the creation of the spheroid as due to the collapse of either a single large gas cloud or several smaller gas lumps. The inclusion of gas infall makes the SFR start at a lower value than in the closed box case, reach a maximum and then decrease as the gas is used up.

The infall term gives the rate at which primordial gas is accreted by the protogalaxy. The adopted expression is

$$\left[ \frac{dG_i(t)}{dt} \right]_{\text{infall}} = X_{i,\text{infall}} C e^{-(t/\tau)}, \quad (2)$$

where  $G_i(t)$  is the mass density of element  $i$  at time  $t$  and  $X_{i,\text{infall}}$  describes the chemical composition of the accreted gas, which is assumed to be primordial.  $C$  is a constant obtained by integrating the infall law over time and requiring that  $\sim 90$  per cent of the initial gas has been accreted at  $t_{\text{gw}}$  (in fact, we halt the infall of the gas at the onset of the galactic wind). Finally,  $\tau$  is the infall time-scale.

In order to compare our predicted abundances with the observed ones, we must compute the mean stellar abundance of the element  $X$  ( $\langle Z_X \rangle \equiv \langle Z_X \rangle$ ), defined as (Pagel & Patchett 1975):

$$\langle Z_X \rangle = \frac{1}{S_0} \int_0^{S_0} Z_X(S) dS, \quad (3)$$

where  $S_0$  is the total mass of stars ever born contributing to the light at  $z = 0$ . For massive ellipticals, results obtained by averaging over the stellar mass are very close to those obtained by averaging over the stellar luminosity at  $z = 0$  (the difference for the models presented in this paper is typically less than 0.05 dex), since the indices are weighted by  $V$ -band luminosity (see e.g. Matteucci, Ponzoni & Gibson 1998).

#### 3.2 General overview of the models

We run models for elliptical galaxies with masses  $10^{10}$  and  $10^{12} M_\odot$ . The basic features common to all models are listed in Table 1, where the input luminous mass, effective radius, star formation efficiency, infall time-scale and time of the galactic wind onset are listed in columns 1–5, respectively.  $M_{\text{lum}}$  is the *nominal* mass of the object, i.e. the mass of the initial gas cloud, with the infall law normalized such that 90 per cent of the mass is accreted between  $t = 0$  and  $t \sim t_{\text{gw}}$ . The mass in stars at  $z = 0$  is  $\sim 0.2$ – $0.4 M_{\text{lum}}$  for all models and the velocity dispersion  $\sigma$  is evaluated from the relation  $M = 4.65 \times 10^5 (\sigma/\text{km s}^{-1})^2 (R_{\text{eff}}/\text{kpc}) M_\odot$  (Burstin et al. 1997). The effective radius  $R_{\text{eff}}$  is the final one, achieved when the collapse is over.

**Table 1.** Summary of model properties: physical quantities.

$M_{\text{lum}}$ ( $M_\odot$ )	$R_{\text{eff}}$ (kpc)	$\nu$ ( $\text{Gyr}^{-1}$ )	$\tau$ (Gyr)	$t_{\text{gw}}$ (Gyr)
$10^{10}$	1	3	0.5	1.30
$10^{12}$	10	22	0.2	0.44

Parameters such as the star formation efficiency ( $\nu$ ), the infall time-scale ( $\tau$ ), the IMF and the fraction of binary systems that give rise to a Type Ia SN explosion have been taken to be the same as in the best model of PM04. The latter authors show that these choices lead to good agreement with a large set of optical observables. In the present work, we can study for the first time the chemical evolution in much finer detail. The modifications to the standard PM04 nucleosynthesis presented here are modest adjustments affecting Ca, C and N abundances. They do not alter the satisfactory agreement between the observations discussed in PM04 and their best model predictions.

### 3.3 Stellar yields

Although in the present work we will discuss only Mg, Fe, Ca, N and C, our code follows in detail the evolution of 21 chemical elements, for which we need to adopt detailed stellar nucleosynthesis prescriptions.

We first define a *fiducial* model (model PM04) with the same nucleosynthesis prescriptions as in PM04.

(i) For single low- and intermediate-mass stars ( $0.8 \leq M/M_{\odot} \leq 8$ ) we make use of the yields of van den Hoek & Groenewegen (1997, hereafter vdHG) as a function of metallicity, with the mass-loss parameter  $\eta_{\text{AGB}}$  dependent on the metallicity as follows:  $\eta_{\text{AGB}} = 1$  for  $Z = 0.001$ ,  $\eta_{\text{AGB}} = 2$  for  $Z = 0.004$  and  $\eta_{\text{AGB}} = 4$  for  $Z = 0.008, 0.02$  and  $0.04$ . A lower value of  $\eta_{\text{AGB}}$  implies a larger yield of carbon because lower mass-loss rates lead to longer stellar lifetimes and hence to more thermal pulses. As a consequence, more C is dredged up to the stellar surface (see Chiappini et al. 2003b).

(ii) For massive stars ( $M > 8 M_{\odot}$ ) we adopt the yields of Thielemann, Nomoto & Hashimoto (1996, hereafter TNH96) computed for the solar chemical composition. With this choice of stellar yields, the N from massive stars has a secondary origin,<sup>2</sup> whereas a fraction of the N coming from low- and intermediate-mass stars has primary origin (vdHG).

(iii) Finally, we use the yields of Nomoto et al. (1997, model W7) for Type Ia SN. These are assumed to originate from C–O white dwarfs in binary systems that have accreted material from a companion (the secondary), reached the Chandrasekar mass, and exploded via C deflagration.

In the next sections we will also modify the base model to include other nucleosynthesis prescriptions. For C, N, and O the above fiducial model will be compared with models computed using the stellar yields of the Geneva group, which include the effects of both mass loss and rotation. The adopted yields are the same as the ones adopted by Chiappini et al. (2006a), where details can be found. Briefly, the yields of MM02 were adopted for metallicities larger than  $Z = 10^{-5}$  over the whole mass range, assuming a rotational velocity of  $300 \text{ km s}^{-1}$ . Below this value we adopted the yields of H07 for massive stars, while keeping the MM02 calculations for low- and intermediate-mass stars. For Type Ia SN we kept the same prescription as in PM04 model.

The different cases studied here, with different stellar evolution prescriptions, are summarized below and in Table 2.

<sup>2</sup> A secondary element is a chemical species which is created from the metals originally present in the composition of a given star. In the simple model for chemical evolution (e.g. Matteucci 2001) it has been shown that the mass abundance in the gas of a secondary element evolves as the square of the total metallicity.

**Table 2.** Summary of model properties: stellar yields.

Model	Yields for C,N	
	low- and intermediate-mass stars	Massive stars
PM04	vdHG	TNH96
Model I	vdHG	H07 for $Z < 10^{-8}$ MM02 otherwise
Model IZ	vdHG	H07
Model II	MM02	H07 for $Z < 10^{-8}$ MM02 otherwise
Model IIZ	MM02	H07 for $Z < 0.004$ MM02 otherwise

(i) Model I: as PM04, but the CNO yields for massive stars ( $m > 8 M_{\odot}$ ) are as in Chiappini et al. (2006a).

(ii) Model IZ: as model I, except that for CNO we adopt the yields for massive stars at  $Z = 10^{-8}$  (H07) as if they were valid for the entire metallicity range. The effect is to increase the output yields of C and N over those of model I. Although this is clearly not physically justified, we use this model to illustrate the effect of boosting C and N.

(iii) Model II: in this case, we adopted the nucleosynthesis prescriptions for CNO used in Chiappini et al. (2006a) for the full stellar mass range.

(iv) Model IIZ: as model II, but here the H07 yields for massive stars are adopted for  $Z < 0.004$ . This could apply to systems with high SFRs such as ellipticals, where the number of fast rotators could have been larger, extending to larger metallicities than in the MW (see Decressin et al. 2007 for the same suggestion in the case of globular clusters).

## 4 RESULTS

In Table 3 we present the mass-weighted average stellar abundance ratios (cf. equation 3) predicted by each of the models described in the previous section. In the following sections, we analyse each of the models in detail. We first focus on Mg and Ca, whose

**Table 3.** Mass-weighted stellar abundance ratios.

$M_{\text{lum}}$ ( $M_{\odot}$ )	[(Mg/Fe)]	[(Fe/H)]	[(Ca/Fe)]	[(C/Fe)]	[(N/Fe)]
PM04					
$10^{10}$	0.15	0.03	−0.07	−0.55	−0.19
$10^{12}$	0.30	0.16	0.04	−0.5	−0.18
Model I					
$10^{10}$	0.15	0.03	−0.07	−0.02	−0.05
$10^{12}$	0.30	0.16	0.04	0.14	−0.01
Model IZ					
$10^{10}$	0.15	0.03	−0.07	0.22	0.02
$10^{12}$	0.30	0.16	0.04	0.34	0.09
Model II					
$10^{10}$	0.15	0.03	−0.07	−0.002	−0.34
$10^{12}$	0.30	0.16	0.04	0.154	−0.19
Model IIZ					
$10^{10}$	0.15	0.03	−0.07	0.09	−0.27
$10^{12}$	0.30	0.16	0.04	0.236	−0.14

abundances are well reproduced by the PM04 model without any further modification of the stellar yields. We then discuss C and N.

## 4.1 Mg and Ca

### 4.1.1 $[(\text{Mg}/\text{Fe})]$

The analysis of the mass– $[(\text{Mg}/\text{Fe})]$  relation has been comprehensively addressed in PM04, Pipino & Matteucci (2006, 2008) and Pipino, Silk & Matteucci (2009), where a detailed comparison with the observations has been made. The Graves et al. (2007) observational result for this abundance ratio is remarkably similar to previous work (e.g. Bernardi et al. 2003; Nelan et al. 2005; Smith et al. 2006), therefore, we do not repeat the analysis here. We just recall that an overabundance of Mg relative to Fe is the key indicator that galaxy formation occurred before a substantial number of Type Ia SNe could explode and contribute to lower the  $[(\text{Mg}/\text{Fe})]$  ratio (for the time-delay model, see Matteucci 2001). In addition, the  $[(\text{Mg}/\text{Fe})]$  ratio in the cores of ellipticals increases with galactic mass (Worthey, Faber & Gonzalez 1992; Weiss, Peletier & Matteucci 1995; Nelan et al. 2005). This relation seems to be already in place at redshift 0.4 (Ziegler et al. 2005).

In order to account for this trend in the star formation time-scale there are at least three possibilities that have been discussed in the literature. One involves the loss of residual gas via galactic winds that are initiated earlier in the most massive objects (the *inverse wind* picture, see Matteucci 1994). Another possibility is to assume an IMF which becomes systematically flatter with increasing galactic mass. A selective loss of metals could also be the cause for the increase of  $[(\text{Mg}/\text{Fe})]$  in more massive galaxies (see Matteucci et al. 1998). We consider the first possibility to be the best motivated, and we will refer to it as *chemical downsizing*. Maiolino et al. (2008) have presented observational evidence for chemical downsizing as far back as  $z \sim 3$ .

Recently Pipino et al. (2009) showed that a more physically motivated value for  $\nu$  gives results in excellent agreement with the observations (and with PM04). In particular, following Silk (2005), they argue that a short ( $10^6$ – $10^7$  yr) super-Eddington phase can provide the accelerated triggering of star formation needed. The subsequent quenching of star formation is accomplished by the SN energy input and results in the usual black hole mass–spheroid velocity dispersion relation (Magorrian et al. 1998).

The observational scatter in the relation between  $[(\text{Mg}/\text{Fe})]$  and galactic mass can be entirely explained as intrinsic scatter. Local effects, such as variations in the SN feedback efficiency of the order of a factor of 2 with respect to the best model case, can induce or delay the onset of the galactic wind and thus contribute to setting the final value for  $[(\text{Mg}/\text{Fe})]$ .

On the other hand, such a relation cannot be explained by a sequence of dry-mergers that create a massive spheroid starting from low-mass  $\alpha$ -enhanced building blocks without violating other fundamental constraints (Pipino & Matteucci 2008).

The PM04 best model predicts  $d[(\text{Mg}/\text{Fe})]/d \log \sigma = 0.37$ , in excellent agreement with the reported value of 0.36 by Graves et al. (2007). This abundance ratio was used by PM04 as a crucial constraint in order to set all the relevant physical quantities reported in Table 1. The same values are adopted here so that models I, IZ, II and IIZ also obey to this fundamental constraint.

In the following sections we study other abundance ratios and, when a discrepancy is found between model predictions and the observations, the problem is addressed by comparing model predictions computed with different stellar yield prescriptions.

### 4.1.2 $[(\text{Ca}/\text{Fe})]$

The observations show that, although Ca belongs to the group of the  $\alpha$  elements, the strength of the observed Ca lines appear to follow  $[(\text{Fe}/\text{H})]$  instead of  $[(\text{Mg}/\text{H})]$  (Trager et al. 1998; Worthey 1998; Saglia et al. 2002). In particular Thomas, Maraston & Bender (2003) suggested  $[(\text{Ca}/\text{Mg})] = -0.15$ , and Saglia et al. (2002), after a detailed analysis of several possible sources of error, claimed that the Ca depletion in ellipticals is real. Such a result is confirmed by Graves et al. (2007), who find the  $[(\text{Ca}/\text{Fe})]$  ratio to be nearly solar over the entire galactic mass range.

The PM04 calculations already suggested  $[(\text{Ca}/\text{Mg})] = -0.152$  and  $[(\text{Ca}/\text{Fe})] = -0.03$  (these values are for the core of a  $10^{11} M_{\odot}$  PM04 galaxy) and are in excellent agreement with the above-mentioned observations. Here we add that at either lower or higher galactic masses the predicted ratio is close to the solar value with a very mild relation with mass. A linear regression fit of the mass weighted stellar abundance ratio as a function of the stellar velocity dispersion returns  $d[(\text{Ca}/\text{Fe})]/d \log \sigma = 0.27$  for PM04 (and hence the same value for models I, IZ, II and IIZ), steeper than the slope of 0.13 reported by Graves et al. (2007). We notice that if we adopt Woosley & Weaver (1995) yields for massive stars we obtain  $d[(\text{Ca}/\text{Fe})]/d \log \sigma = 0.18$ , which is in better agreement with the observed slope but produces  $[(\text{Ca}/\text{Fe})]$  values offset about 0.15 dex higher than observations at a given mass.

As shown in PM04, this result can be explained simply by SN yields. In fact, the  $\alpha$ -elements exhibit different degrees of enhancement with respect to Fe in the results of the chemical evolution model (see François et al. 2004). This is due, from a theoretical point of view, to the different degree of production of each element in Type II and Type Ia SNe. In particular, Ca and Si show a lower overabundance relative to Fe than O and Mg, since they are also produced substantially in Type Ia SNe. In fact, the mass of Ca ejected during a Type Ia SN explosion in the model W7 (Nomoto et al. 1997) is  $\sim 0.012 M_{\odot}$ , whereas the contribution of a typical Type II SNe (averaged over a Salpeter IMF in the mass range 10–50  $M_{\odot}$ ) is  $\sim 0.0058 M_{\odot}$  (see table 3 of Iwamoto et al. 1999). While some fine-tuning of the stellar nucleosynthesis could improve even further the agreement with observations, we stress that PM04 explains the behaviour of the Ca abundance as a function of mass without requiring changes in the adopted chemical evolution model parameters.

## 4.2 C and N

Figs 1 and 2 show our model predictions for the  $[(\text{C}, \text{N}/\text{Fe})]$ –mass relations compared with the observed ones by Graves et al. (2007) (represented by pentagons connected by a solid line). The PM04 model (triangles joined by a solid line) predicts both  $[(\text{C}/\text{Fe})]$  and  $[(\text{N}/\text{Fe})]$  to be below solar and to show no dependence on galactic mass, at variance with the observations. The other models (i.e. I: dotted line; IZ: dashed line; II: long-dashed line; IIZ: long-dashed–dot line), while keeping the same star formation history as PM04, show different trends in abundance ratios with mass, reflecting the different assumptions about the nucleosynthesis. Most of the modified models lead to an improvement over the predictions of PM04. Thus, for the first time we can use local elliptical galaxies as a test bench for stellar nucleosynthesis studies. In the following sections we will discuss the C and N results in further detail.

#### 4.2.1 $[(C/Fe)]$ in the integrated stellar spectrum

We first focus on the predictions of our new models concerning the  $[(C/Fe)]$  abundance ratio in Fig. 1. Model I (dotted line) predicts  $d[(C/Fe)]/d \log \sigma = 0.4$ , in good agreement with the value of 0.5 reported by Graves et al. (2007, solid line). However, this model has a zero-point of the mass- $[(C/Fe)]$  relation  $\sim 0.1$  dex smaller than the observed one.

The large difference between model I and PM04 is due to the larger contribution of massive stars to the carbon production in the case of the Geneva group yields with respect to the TNH96 ones. The larger C yields of the Geneva group are found not only at very low metallicities (due to rotation, as explained before) but also at solar metallicities (see fig. 1 of Chiappini et al. 2003b for a comparison of the C yields of the two groups at  $Z = Z_{\odot}$ ). In fact, the mass-loss rate, which increases with metallicity, contribute to increase the overall C yields (see MM02).

A similar result is found for model II (long-dashed line), which differs from model I only in the C yields for intermediate-mass stars (vdHG in model I and MM02 in model II). The difference between these two models is expected to be small since, as shown by Chiappini et al. (2003a), the yields of C from vdHG and MM02 for low- and intermediate-mass stars are similar. In fact, although MM02 yields do not include the third dredge up contribution, they obtain a similar effect thanks to rotation and mass loss (see Chiappini et al. 2003a for details).

Model IZ (dashed line) predicts:  $d[(C/Fe)]/d \log \sigma = 0.3$  with a larger zero-point. In this case the model galaxies are more C enhanced than the observed ones. This is not surprising, as model IZ assumes fast rotators to exist at all metallicities and not only below  $Z = 10^{-8}$  as done in Chiappini et al. (2006a). This illustrates the effect of substantial additional C enhancement from massive stars but is not based on any physical motivation.

Finally, model IIZ matches the  $[(C/Fe)]$ -mass relation quite well. In this case, the C contribution from fast rotators is extended up to  $Z = 0.004$  and is therefore larger than in model II (where fast rotators exist only up to  $Z = 10^{-8}$ , see Section 3.3).

Overall, it is encouraging that all of the models which include the effects of rotation and mass loss in massive stars (models I, IZ, II and IIZ) produce reasonable agreement with the data, showing the correct slope of the mass- $[(C/Fe)]$  relation, with zero-point offsets of the order of only  $\pm 0.1$  dex from the data. There are variations depending on the various yield tables adopted, but these variations are relatively small. This suggests that modelling of the nucleosynthesis of C in massive rotating stars might approach a consensus soon and therefore that C abundances will be a powerful new tool for constraining galaxy star formation histories.

It should be kept in mind that the transformation of Lick indices into mean stellar abundances carries uncertainties, as discussed in Section 2.2. These uncertainties are more likely to affect the zero-point calibration of the abundances, while the *relative* abundances and therefore the abundance trends with  $\sigma$  should be fairly robust. Finally, we notice that both our model predictions and the data set of Graves et al. (2007) are at odds with the recent claim (Clemens et al. 2006) of a decrease in the  $[(C/H)]$  value in stars as function of the galactic mass.

#### 4.2.2 $[(N/Fe)]$ in the integrated stellar spectrum

Concerning N, models I and IZ (see Fig 2, symbols as in Fig. 1), substantially increase the zero-point of the mass- $[(N/Fe)]$  relation with respect to PM04, hence improving the agreement with

the observations. However, both models predict a rather flat slope:  $d[(N/Fe)]/d \log \sigma = 0.1$  (a factor of 5 flatter than the value indicated by the SDSS galaxies). We remind the reader that models I and IZ assume primary N production in massive stars, whereas in PM04 the N from massive stars is only secondary.

On the other hand, model II is able to predict a slope ( $d[(N/Fe)]/d \log \sigma = 0.4$ ) for the mass- $[(N/Fe)]$  relation, in much better agreement with Graves et al.'s findings, but it does not improve upon the original PM04 model in terms of the absolute value. In fact,  $[(N/Fe)]$  is underpredicted by 0.4 dex (i.e. more than a factor of 2) in this case. The only differences between models I and II are the adopted yields for low- and intermediate-mass stars. Model I was computed with the yields of vdHG, which predict larger quantities of N than the yields of MM02 (adopted in model II). These large N quantities are responsible for both the larger zero-point and the flatter behaviour of the mass- $[(N/Fe)]$  relation. When assuming that the fast rotators play a role up to metallicities  $Z = 0.004$  (model IIZ), the  $[(N/Fe)]$  zero-point is increased by  $\sim 0.1$  dex, which is still not enough to account for the observed values.

In the case of models II and IIZ, the differences between observed and predicted values at a given galactic mass are probably too large to be explained in terms of either uncertainties in the calibration of the Lick system (see Section 2.2), or in the actual measurements. This offset is larger than the  $3\sigma$  measurement error quoted in Graves et al. (2007) for the observed zero-point of the  $[(N/Fe)]$ - $\sigma$  relation.

It is worth noting that, unlike in the case with  $[(C/Fe)]$ , there is substantial disagreement in the predicted values of  $[(N/Fe)]$  between the four models, both in the predicted values of  $d[(N/Fe)]/d \log \sigma$  and in the zero-points (at the level of 0.4 dex). This indicates that the various nucleosynthesis yield predictions for N vary significantly between groups and are highly sensitive to the mass and metallicity range over which rotation is assumed to be relevant. The nucleosynthetic predictions for N are therefore significantly less secure than those for C.

Furthermore, as discussed in Section 2.2, stellar  $[(N/Fe)]$  abundance ratio measurements in the observed galaxies are more uncertain than the other abundance determinations.

#### 4.2.3 N abundance in the gas: model ellipticals

Since the predicted values for  $[(C, N/Fe)]$  are the result of the convolution of the temporal evolution of  $[C, N/Fe]$  in the gas with the SFR, it is important to study the gas abundances in order to understand the differences between the models presented in the previous section. In Fig. 3 we plot the evolution of  $[N/Fe]$  in the gas phase of the  $10^{10}$  and the  $10^{12} M_{\odot}$  model galaxies (left- and right-hand panels, respectively) as a function of  $[Fe/H]$ . The dotted lines mark relevant times during the course of star formation in the galaxy, including the metallicity at the time when the SFR reaches its peak, the metallicities at which the SFR is within a factor of 2 from the peak value, and the onset of the galactic wind (labelled as  $t_{\text{gw}}$ ). This event sets the time (hence the metallicity) at which the star formation stops. This illustrates the values of  $[N/Fe]$  at which most of the stars in each galaxy are formed.

First of all, a comparison of Figs 2 and 3 shows that, even if N is more enhanced in more massive (hence more metal rich) galaxies, this does not imply that N has a secondary origin! It is true that models in which N is mostly secondary (e.g. PM04) have gas phase  $[N/Fe]$  abundances which increase steeply with  $[Fe/H]$ , as shown in Fig. 3 (PM04 is the solid black line). However, this does not necessarily translate into a strong  $[(N/Fe)]$ -mass relation (see Fig. 2).

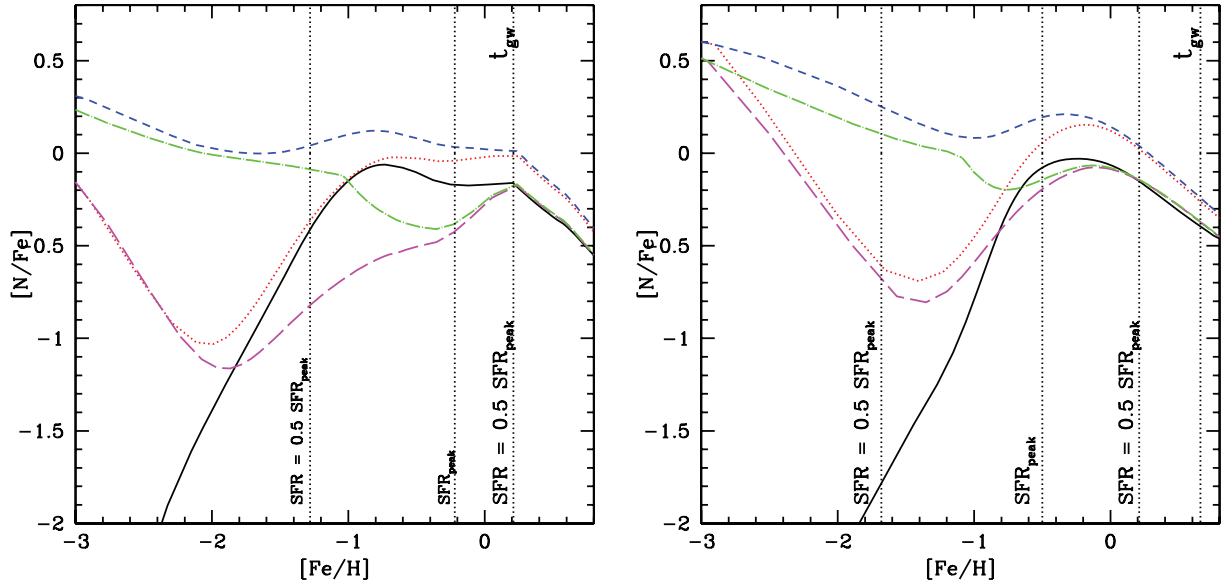


**Figure 3.**  $[N/Fe]$  as a function of  $[Fe/H]$  in the gas for a  $10^{10} M_{\odot}$  (left-hand panel) and for a  $10^{12} M_{\odot}$  (right-hand panel) elliptical galaxy. Different lines represent the different models in Table 2: PM04 (solid line) and models I (dotted line), IZ (dashed line), II (long-dashed line) and IIZ (short-dash–dotted line). Vertical dotted lines indicate the metallicity where the SFR reaches its peak, as well as when it rises to and drops by a factor of 2 from this value. Also shown is the metallicity at the onset of the galactic wind (labelled as  $t_{\text{gw}}$ ), indicating the time (hence the metallicity) at which the star formation stops. This illustrates the values of  $[N/Fe]$  at which most of the stars in each galaxy are formed.

In contrast, models which produce a better match to the observed  $[N/Fe]$ –mass relation (e.g. model IZ, dashed blue line), include substantial primary N production in massive stars and show high gas-phase  $[N/Fe]$  abundances at low  $[Fe/H]$  (Fig. 3).

By comparing the left-hand panel of Fig. 3 ( $10^{10} M_{\odot}$  case) to the right-hand panel ( $10^{12} M_{\odot}$  case), it is clear that the more massive galaxy features a higher  $[N/Fe]$  ratio in the gas during the phases when the star formation proceeds at its maximum rate. Stars form out of this enriched material until the onset of the galactic wind at time  $t_{\text{gw}}$ . The difference between the  $10^{10}$  and  $10^{12} M_{\odot}$  galaxies is the smallest for the PM04 model, hence we predict a rather flat slope in the  $[N/Fe]$ –mass relation. The difference is largest in models II and IIZ, which therefore exhibit the steepest slope in the  $[N/Fe]$ –mass relation (Fig. 2).

This result is quantified in Fig. 4 for model IIZ: the normalized distribution of stars as a function of  $[N/Fe]$  peaks at higher values of the abundance ratio and features a smaller tail at  $[N/Fe] < -1$  in the  $10^{12} M_{\odot}$  model galaxy (full histogram) than in the  $10^{10} M_{\odot}$  galaxy (empty histogram). Note that the values of  $[N/Fe]$  derived by means of equation (3) and shown in Table 3 correspond to the *mean value* of distributions like the one shown in Fig. 4. The mean does not always coincide with the peak value (i.e. the *mode*) of the distribution. Given the asymmetry of the distributions, the mean, in fact, tends to be  $\sim 0.1$ – $0.2$  dex lower than the mode. By comparing the distribution of stars as a function of  $[N/Fe]$  for different models, we can also explain the differences in the predicted  $[N/Fe]$  at a given mass (Section 4.2.2). For instance, model IZ features a distribution which peaks at higher  $[N/Fe]$  and has a larger mean value than model PM04. Finally, we note that all the models shown in Fig. 3 (with the exception of models IZ and IIZ) exhibit a  $[N/Fe]$  ratio below solar during most of the galaxy evolution.

Intermediate-mass stars (i.e.  $M < 8 M_{\odot}$ ) do not contribute metals to the ISM until  $\sim 30$  Myr after the beginning of star formation. This corresponds to  $Z = 5 \times 10^{-4}$  in the  $10^{10} M_{\odot}$  galaxy and  $Z = 3 \times$

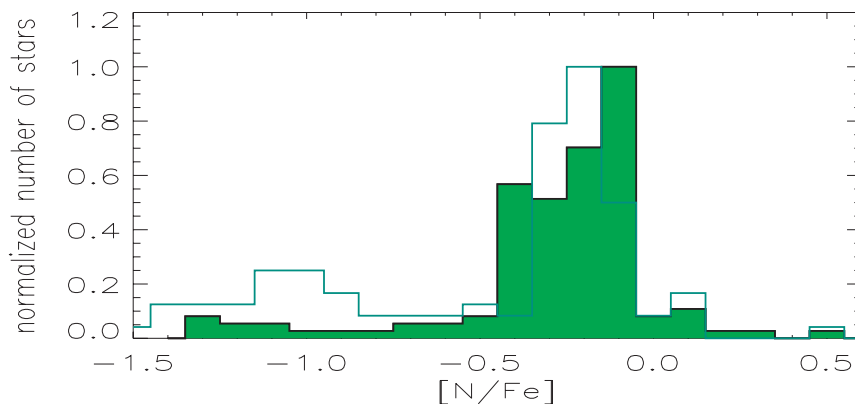
$10^{-3}$  in the  $10^{12} M_{\odot}$  galaxy, where the evolution is faster. Because of the very short time-scale of galaxy formation (see Table 1), the lowest stellar mass which can contribute to the chemical enrichment of the model galaxies is  $\sim 1.6 M_{\odot}$  in the  $10^{10} M_{\odot}$  case and  $\sim 2 M_{\odot}$  in the  $10^{12} M_{\odot}$  case. The differences in the N production at low metallicities (i.e.  $[Fe/H]$  and  $[O/H] < -2$ ) will have little effect in the final  $[N/Fe]$  ratio because very few stars are formed at these metallicities.

#### 4.2.4 N abundance in the gas: high-redshift progenitors

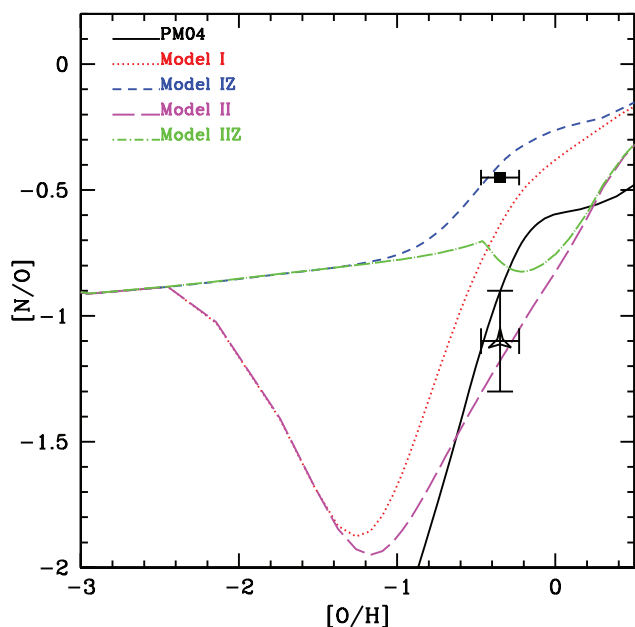
Ideally, one would use gas-phase abundance ratios as shown in Fig. 3 to further refine the model. Unfortunately, no such measurements exist in low-redshift ellipticals, as they are almost devoid of gas. In order to perform such an exercise we must resort to high-redshift objects, such as the Lyman break galaxy (LBG) MS 1512–cB58 (Teplitz et al. 2000; Pettini et al. 2002). This is currently the brightest LBG known, because it is gravitationally lensed. The LBG is at  $z = 2.7672$  and has a luminous mass of  $\sim 10^{10} M_{\odot}$  with a SFR of  $\sim 40 M_{\odot} \text{ yr}^{-1}$  (Pettini et al. 2002). We use this galaxy because, from the analysis of its properties and its chemical abundance pattern, Matteucci & Pipino (2002) suggest MS 1512–cB58 to be a low-mass young elliptical experiencing its main episode of star formation and galactic wind.

Fig. 5 shows the evolution of the  $[N/O]$  abundance ratio as function of  $[O/H]$  in the gas for our model galaxy with  $M_{\star} = 10^{10} M_{\odot}$ , for each of the nucleosynthesis cases studied in the previous sections. In this figure, the point with error bars represents the LBG.<sup>3</sup>

<sup>3</sup> Note that the N abundance is inferred from absorption lines (Pettini et al. 2002), whereas the O abundance comes from emission line measurements (Teplitz et al. 2000).



**Figure 4.** Normalized number of stars as a function of  $[N/Fe]$  for model IIZ in the case of the  $10^{10} M_{\odot}$  model galaxy (empty histogram) and of the  $10^{12} M_{\odot}$  model (filled histogram).



**Figure 5.**  $[N/O]$  as a function of  $[O/H]$  in the gas for the different  $10^{10} M_{\odot}$  models: PM04 (solid line) and models I (dotted line), IZ (dashed line), II (long-dashed line) and IIZ (short-dash-dotted line). The triangle with error bars is the observed value for the LBG MS 1512–cB58 (Pettini et al. 2002), whereas the solid square is the estimate from Teplitz et al. (2000).

The models shown in Fig. 5 have SFRs similar to the one observed in MS 1512–cB58. The solid line represents the original PM04 model. The  $[N/O]$  abundance ratio rises quite steeply with metallicity<sup>4</sup> because, in the PM04 model, the N from massive stars is assumed to be a secondary element. The predictions of the PM04 model (which is an improved version of the chemical evolution model presented by Matteucci & Pipino 2002) are within  $1\sigma$  of the observed value.

Model II (long-dashed line) performs equally well, exhibiting an early (i.e.  $[O/H] < -3$ ) plateau with values around  $[N/O] = -1$ , followed by a decrease due to the metallicity-dependent yields

of massive stars. Later, intermediate-mass stars start contributing to the chemical enrichment (once  $[O/H] > -1$  dex in the case shown in Fig. 5). Such a contribution starts to be important around  $[O/H] = -0.5$ , where a new rise in the  $[N/O]$  ratio is observed.

The detailed behaviour of the curve predicted by model II is still uncertain, primarily due to the following reasons. (a) There are still no complete grids of stellar yields for models with rotation. Here we are combining the calculations of MM02 for  $300 \text{ km s}^{-1}$  with the more recent calculations of H07, which includes the fast rotators ( $500\text{--}800 \text{ km s}^{-1}$ ). Grids with intermediate values of rotational velocities at different metallicities are currently not available. Moreover, there are small differences between MM02 and H07 calculations, such as different amounts of convective overshooting, that prevent a completely self-consistent approach. (b) The contribution to N by super-AGB stars<sup>5</sup> could be important (Siess 2007). This is not included here as no stellar yield calculations for these objects are available at the moment. These stars would play a role at earlier times than low- and intermediate-mass stars and could contribute to fill up the valley seen in Fig. 5 (also contributing to increase the median value of  $[N/Fe]$  in Fig. 2). (c) In MM02, the intermediate-mass stars were not followed up to the end of their evolution and the contribution of hot bottom burning could be missing (but see Chiappini et al. 2003b).

Despite of the above caveats, the important point here is that model II predicts a high N/O ratio at early phases that later decreases and then increases again. The amount of the decrease in N/O at intermediate metallicities is still uncertain but it clearly shows that some metallicity dependence of the N yields in massive stars is necessary in order to bring  $[N/O]$  back up to levels consistent with the LBG.

On the other hand, models IZ and IIZ, which are built to enhance C and N in order to fit the *stellar* ratios in local ellipticals, predict a large N abundance with respect to O at low  $[O/H]$ . This is because we let massive stars produce N with the same stellar yields as if they were in the lowest metallicity regime. The sudden downturn of model IIZ at  $[O/H] \sim -0.5$  is due to the adopted threshold metallicity for including the fast rotators. This drop is much less important than what happens in model II, where the fast rotators

<sup>5</sup> Super-AGB stars are massive enough to ignite C in a degenerate core but do not proceed into neon burning and beyond. They are thus an intermediate case between intermediate-mass and massive stars.

<sup>4</sup> O contributes 60 per cent of the total metallicity in this system.

contribute during a much shorter period of the evolution of these galaxies. In other words, in model IIZ the drop is just shifted to larger metallicities because we allowed fast rotators to contribute for longer times (up to larger metallicities).

Model I (dotted line) is an intermediate case between PM04 and model II. At variance with the fiducial PM04 model, it features an early enhancement of N owing to the production from low-metallicity massive stars, as in model II. It also shows a steeper rise around  $[O/H] = -0.5$  due to the fact that in this case, vdHG nucleosynthesis for intermediate-mass stars is producing more N (the hot bottom burning contribution).

While models I and IIZ are still marginally consistent with the data from Pettini et al. (2002, triangle in Fig. 5), model IZ – which better matches the  $[(N/Fe)]$ –mass relation – predicts a  $[N/O]$  ratio more than a factor of 3 larger than the observed LBG value at  $[O/H] = -0.35$ . However, the gas-phase N abundance inferred from *emission* lines in the same galaxy is  $[N/O] \sim -0.5$  (Teplitz et al. 2000, full square in Fig. 5), more than three times higher than the  $[N/O]$  inferred from the absorption line measurements of Pettini et al. (2002). Pettini et al. argue that the N abundance inferred from emission lines may be substantially overestimated. None the less, we can interpret the factor of 3 difference in the N abundance between *emission* and *absorption* lines as an estimate of the uncertainty in the gas-phase measurements. Using the Teplitz et al. (2000) emission line abundance brings model IZ into excellent agreement with *both* stellar- and gas-phase abundances (full square in Fig. 5). Unfortunately, they do not provide error bars, therefore, we cannot quantitatively estimate the level of agreement with our model prediction.

It is important to stress that a comparison with a single high-redshift object, which may be a young elliptical caught in the act of formation, may not be appropriate. More data on gas-phase abundances in high-redshift objects are needed to confirm the tension emerging with respect to abundances measured in stars and to reconcile *emission*- and *absorption*-line measurements of the gas-phase abundance. However, along with the observations of DLA (which also show systematically lower N/O ratios than the stars in the MW, again suggesting a  $Z$  dependency of the N yields in massive stars), such a comparison demonstrates the existence of a dichotomy between stellar abundances (which tend to favour higher N abundances) and gas-phase abundances.

Our analysis demonstrates a potential inconsistency between the stellar N abundances observed in local ellipticals and the gas-phase abundances observed in a likely progenitor of these galaxies at higher redshift. The stellar  $[(N/Fe)]$  abundance ratio appears to require substantial N enrichment due to both massive and intermediate-mass stars (e.g. model IZ), but this model produces an  $[N/O]$  abundance ratio that is too high to match the LBG data from Pettini et al. (2002). This discrepancy disappears if the  $[N/O]$  abundance ratio of MS 1512–cB58 is in fact  $[N/O] = -0.5$ , as determined by Teplitz et al. (2000).

Another possible solution to this discrepancy is that the  $[(N/Fe)]$  ratios inferred from stellar spectra are overestimated by about 0.3 dex (this is the amount necessary to bring it into agreement with model prediction and the Pettini et al. LBG data at the same time). The various uncertainties in the  $[(N/Fe)]$  measurements were discussed in Section 2.2. An offset of 0.3 dex is larger than can easily be accounted for in this way, but is certainly not impossible, given the uncertainties in the modelling process, the paucity of good test data, and the fact that these constitute the first attempts to quantify  $[(N/Fe)]$  in unresolved stellar populations.

## 5 CONCLUSIONS

In this paper we have analysed the mass– $[(Ca,C,N/Fe)]$  ratio relations observed in local spheroids by means of a chemical evolution model which successfully reproduces the mass– $[(Mg/Fe)]$  and the mass–metallicity relations (the PM04 model). Our theoretical predictions are compared to the observed relations inferred from integrated spectra of early-type galaxies in SDSS by Graves et al. (2007). We find the following.

(i) The  $[(Ca/Fe)]$ –mass relation is naturally explained by the PM04 best model without any further assumption needed. In particular, the underabundance of Ca with respect to Mg can be attributed to the relative contributions of Type Ia and Type II SNe to the nucleosynthesis of these two elements.

(ii) The standard nucleosynthesis prescriptions adopted by PM04 (i.e. where rotation and mass loss are not taken into account) lead to chemical evolution models in which C traces Fe and N behaves as a secondary element (i.e. there is no primary nitrogen contribution from massive stars). Instead, the abundance ratios measured for the stellar population in local spheroids suggest that both C and N behave more like  $\alpha$ -elements (e.g. Mg) in the sense that the  $[(C, N/Fe)]$  abundance ratios are supersolar and increase with the galactic mass.

(iii) We show that in order to reproduce the  $[(C/Fe)]$ - and  $[(N/Fe)]$ –mass observed relations it is necessary to consider new nucleosynthesis prescriptions, which take into account both the effects of rotation and mass loss (Meynet et al. 2009). These two important physical processes have already proven to be crucial for our understanding of the abundance ratios in metal-poor stars in the Galactic halo (Spite et al. 2005). Indeed, the high N/O, C/O and low  $^{12}C/^{13}C$  ratios observed in stars with  $[Fe/H] < -2.5$  suggest the existence of fast rotating stars in the very early Universe (Chiappini et al. 2006a,b, 2008).

(iv) The various different prescriptions for the effects of rotation and mass loss on the nucleosynthesis of C considered here all produce results that are consistent with the data and with each other. This indicates that the nucleosynthesis of C is now understood well enough and hence C abundances can be used to place constraints on chemical evolution in galaxies. The same level of consensus is not found for N abundances from the various models. This suggests that the nucleosynthesis of N is more sensitive to the differences in stellar evolution models and that the existing yield tables for N are perhaps less reliable than those for C.

(v) Once these new stellar yields are implemented in the PM04 chemical evolution model, a remarkable agreement with the observations is attained (within the observational uncertainties) both for the slope and the zero-point of the mass– $[(C/Fe)]$  relation (model II). This shows that significant amounts of C must be produced in massive stars (and not only in intermediate-mass stars) in order to reproduce the  $[(C/Fe)]$  abundances of massive early-type galaxies.

(vi) The same model reproduces the steep slope observed for the mass– $[(N/Fe)]$  relation in the local universe. This model also provides predictions for N/O ratios in the gas-phase abundance of young spheroids. The models considered here cannot simultaneously predict the high values of  $[(N/Fe)]$  observed in local stellar populations and the low values of  $[N/O]$  observed in the gas phase of LBG MS 1512–cB58. A factor of  $\sim 0.3$  dex is required to resolve this difference. There are significant uncertainties in both the stellar and gas-phase measurements of N, as well as the N yields, all of which may contribute to the observed discrepancy.

In summary the PM04 model, updated to include new nucleosynthetic yields from stellar models which account for stellar rotation and mass loss, can account for the  $[(\text{Mg}, \text{Ca}, \text{C}/\text{Fe})]$ –mass relations observed in local spheroids. Discrepancies may remain in the case of N. However, our best model (model II) might be completely reconciled with observations if *emission*-line gas-phase N abundance of MS 1512–cB58 is considered, rather than the N abundance determined from *absorption*-line measurements. Another way to reconcile the discrepancy is if the  $[(\text{N}/\text{Fe})]$  in the galaxies, inferred from Lick indices, is overestimated by  $\sim 0.3$  dex. If this turns out to be the case, our results suggest that fast stellar rotation at low  $Z$  and large mass-loss rates at higher metallicities in massive stars have an important impact on the chemical evolution of early-type galaxies, as has already been shown for the Milky Way. On the other hand, if the  $[(\text{N}/\text{Fe})]$  ratios inferred for the SDSS galaxies are correct and if the *absorption*-line gas-phase N abundance of MS 1512–cB58 are typical of young spheroids, a tension between observed gas and stellar abundance ratios remains, suggesting that further processes not envisaged in the present work should be taken into account. However, the uncertainties associated with both stellar and gas-phase N abundance measurements, as well as the uncertainties in the nucleosynthesis of N do not allow us to draw firm conclusions.

Finally, we note that, thanks to large sample sizes, high-quality data and improved stellar population models, we are able for the first time to use elliptical galaxies as a test bench for stellar nucleosynthesis studies. At the same time we present several predictions for the evolution of the N/Fe and N/O abundance in the gas that might be tested on high-redshift protogalaxies.

## ACKNOWLEDGMENTS

We wish to thank the referee for the insightful comments that improved the quality of the paper. AP acknowledges financial support from the Oxford University Astor Travel Grant and the hospitality of UC Santa Cruz, where this project was begun, as well as partial support from NSF grant AST-0649899 during the completion of the manuscript. CC acknowledges financial support from Swiss National Science Foundation (SNF). FM acknowledges financial support by the Italian Space Agency through contract ASI-INA F I/016/07/0. FM and CC acknowledge financial support from PRIN2007 (Italian Ministry of Research), Prot.2007JJC53X\_001.

## REFERENCES

Akerman C. J., Carigi L., Nissen P. E., Pettini M., Asplund M., 2004, *A&A*, 414, 931  
 Bernardi M. et al., 2003, *AJ*, 125, 1882  
 Bundy K., Ellis R. S., Conselice C. J., 2005, *ApJ*, 625, 621  
 Burstein D., Faber S. M., Gaskell C. M., Krumm N., 1984, *ApJ*, 287, 586  
 Burstein D., Bender R., Faber S. M., Nolthenius R., 1997, *AJ*, 114, 1365  
 Carollo C. M., Danziger I. J., Buson L., 1993, *MNRAS*, 265, 553  
 Cescutti G., François P., Matteucci F., Cayrel R., Spite M., 2006, *A&A*, 448, 557  
 Chiappini C., Matteucci F., Meynet G., 2003a, *A&A*, 410, 257  
 Chiappini C., Romano D., Matteucci F., 2003b, *MNRAS*, 339, 63  
 Chiappini C., Matteucci F., Ballero S. K., 2005, *A&A*, 437, 429  
 Chiappini C. et al., 2006a, *A&A*, 449, L27  
 Chiappini C. et al., 2006b, in *International Symp. on Nuclear Astrophysics – Nuclei in the Cosmos-IX*, 25–30 June 2006. Proc. of Science (NIC-IX) 080  
 Chiappini C., Ekstroem S., Meynet G., Hirschi R., Maeder A., Charbonnel C., 2008, *A&A*, 479, 9

Clemens M. S., Bressan A., Nikolic B., Alexander P., Annibali F., Rampazzo R., 2006, *MNRAS*, 370, 702  
 Decressin T. et al., 2007, *A&A*, 464, 1029  
 Desselberger K., Calura F., Prochaska J. X., D’Odorico S., Matteucci F., 2007, *A&A*, 470, 431  
 Fabbian D., Nissen P. E., Asplund M., Pettini M., Akerman C., 2009, *A&A*, in press (arXiv:0810.0281)  
 Faber S. M., Worthey G., Gonzalez J. J., 1992, in Barbuy B., Renzini A., eds, *IAU Symp. 149, The Stellar Populations of Galaxies*. Kluwer, Dordrecht, p. 255  
 François P., Matteucci F., Cayrel R., Spite M., Spite F., Chiappini C., 2004, *A&A*, 421, 613  
 Fulbright J. P., McWilliam A., Rich R. M., 2007, *ApJ*, 661, 1152  
 Graves G. J., Schiavon R. P., 2008, *ApJS*, 177, 446  
 Graves G. J., Faber S. M., Schiavon R. P., Yan R., 2007, *ApJ*, 671, 243  
 Greggio L., Renzini A., 1983, *A&A*, 118, 217  
 Hirschi R., 2007, *A&A*, 461, 571 (H07)  
 Iwamoto K., Barchwitz F., Nomoto K., Kishimoto N., Umeda H., Hix W. R., Thielemann F. K., 1999, *ApJS*, 125, 439  
 Lanfranchi G. A., Matteucci F., Cescutti G., 2006, *A&A*, 453, 67  
 Lanfranchi G. A., Matteucci F., Cescutti G., 2008, *A&A*, 481, 635  
 Magorrian J. et al., 1998, *AJ*, 115, 2285  
 Maiolino R. et al., 2008, *A&A*, 488, 463  
 Mannucci F., Maoz D., Sharon K., Botticella M. T., Della Valle M., Gal-Yam A., Panagia N., 2008, *MNRAS*, 383, 1121  
 Matteucci F., 1994, *A&A*, 288, 57  
 Matteucci F., 2001, *The Chemical Evolution of the Galaxy*. Kluwer, Dordrecht  
 Matteucci F., Greggio L., 1986, *A&A*, 154, 279  
 Matteucci F., Pipino A., 2002, *ApJ*, 569, L69  
 Matteucci F., Ponzzone R., Gibson B. K., 1998, *A&A*, 335, 855  
 Meynet G., Maeder A., 2002, *A&A*, 390, 561 (MM02)  
 Meynet G., Ekström S., Maeder A., 2006, *A&A*, 447, 623  
 Meynet G., Chiappini C., Georgy C., Pignatari M., Hirschi R., Ekström S., Maeder A., 2009, in Andersen J., Bland Hawthorn J., Nordström B., eds, *IAU Symp. 254, The Galaxy Disk in Cosmological Context*. Cambridge Univ. Press, Cambridge, p. 325  
 Nelan J. E., Smith R. J., Hudson M. J., Wegner G. A., Lucey J. R., Moore S. A. W., Quinney S. J., Suntzeff N. B., 2005, *ApJ*, 632, 137  
 Nomoto K., Hashimoto M., Tsujimoto T., Thielemann F. K., Kishimoto N., Kubo Y., Nakasato N., 1997, *Nucl. Phys. A*, 621, 467  
 Pagel B. E. J., Patchett B. E., 1975, *MNRAS*, 172, 13  
 Pettini M., Rix S. A., Steidel C. C., Adelberger K. L., Hunt M. P., Shapley A. E., 2002, *ApJ*, 569, 742  
 Pettini M., Zych B. J., Steidel C. C., Chaffee F. H., 2008, *MNRAS*, 385, 2011  
 Pipino A., Matteucci F., 2004, *MNRAS*, 347, 968 (PM04)  
 Pipino A., Matteucci F., 2006, *MNRAS*, 365, 1114  
 Pipino A., Matteucci F., 2008, *A&A*, 486, 763  
 Pipino A., Matteucci F., Borgani S., Biviano A., 2002, *New Astron.*, 7, 227  
 Pipino A., Silk J., Matteucci F., 2009, *MNRAS*, 392, 475  
 Pompeia L. et al., 2008, *A&A*, 480, 379  
 Saglia R. P., Maraston C., Thomas D., Bender R., Colless M., 2002, *ApJ*, 579, 13  
 Salpeter E. E., 1955, *ApJ*, 121, 161  
 Sanchez-Blazquez P., Gorgas J., Cardiel N., Cenarro J., 2003, *ApJ*, 590, 91  
 Schiavon R. P., 2007, *ApJS*, 171, 146  
 Siess L., 2008, in Charbonnel C., Zahn J. P., eds, *EAS Publ. Ser. Vol. 32, Stellar Nucleosynthesis: 50 Years After B<sup>2</sup>FH Aussois*, France, December 4–8, 2006. EDP Sciences, Les Ulis, p. 131  
 Silk J., 2005, *MNRAS*, 364, 1337  
 Smith R. J., Hudson M. J., Lucey J. R., Nelan J. E., Wegner G. A., 2006, *MNRAS*, 369, 1419  
 Spite M., Decressin T., Meynet G., Charbonnel C., Prantzos N., Ekström S., 2005, *A&A*, 430, 655  
 Strauss M. A. et al., 2002, *AJ*, 124, 1810  
 Teplitz H. I. et al., 2000, *ApJ*, 533, 65  
 Thielemann F. K., Nomoto K., Hashimoto M., 1996, *ApJ*, 460, 408 (TNH96)

- Thomas D., Maraston C., Bender R., 2003, MNRAS, 339, 897  
Toloba E., Sanchez-Blazquez P., Gorgas J., Gibson B. K., 2009, ApJ, 691, 95  
Trager S. C., Worthey G., Faber S. M., Burstein D., Gonzalez J. J., 1998, ApJS, 116, 1  
Trager S. C., Faber S. M., Worthey G., Gonzalez J. J., 2000a, AJ, 119, 1654  
Trager S. C., Faber S. M., Worthey G., Gonzalez J. J., 2000b, AJ, 120, 165  
van den Hoek L. B., Groenewegen M. A. T., 1997, A&AS, 123, 305 (vdHG)  
Weiss A., Peletier R. F., Matteucci F., 1995, A&A, 296, 73  
Woosley S. E., Weaver T. A., 1995, ApJS, 101, 181  
Worthey G., 1998, PASP, 110, 888  
Worthey G., Faber S. M., Gonzalez J. J., 1992, ApJ, 398, 69  
York D. G. et al., 2000, AJ, 120, 1579  
Ziegler B. L., Thomas D., Bohm A., Bender R., Fritz A., Maraston C., 2005, A&A, 433, 519

This paper has been typeset from a  $\text{\TeX}/\text{\LaTeX}$  file prepared by the author.